

Damage Analysis of Biocomposite Laminates Using Model Order Reduction

Gil Ho Yoon¹ and Heung Soo Kim^{2,*}

¹*School of Mechanical Engineering, Hanyang University, Seoul 133-791, Republic of Korea*

²*Department of Mechanical, Robotics and Energy Engineering, Dongguk University-Seoul,
Seoul 100-715, Republic of Korea*

The transient quasi-static Ritz vector method (TQSRV) is applied to efficiently calculate the transient response of a delaminated biocomposite laminate. Delamination of the laminated biocomposite structure was modeled using an improved layerwise displacement field. The piezoelectric coupling effect was modeled using higher order electric potential. One piezoelectric actuator was used to excite the laminated biocomposite plate, and one piezoelectric sensor was used to detect the transient structural response of the plate. Single discrete delamination was seeded in the laminated biocomposite plate, to investigate the effect of delamination. Three different locations of delamination through the thickness direction were considered, to study the effects of delamination on structural response. The Newmark-beta algorithm and the model order reduction (MOR) method were used, to obtain transient response of the delaminated composite plate under impulse loading. The effects of delamination were clearly observed in the power spectral density of the piezoelectric sensor output. From the results, it is concluded that the MOR is a very efficient method in predicting the damage effects of delaminated biocomposite structures.

Keywords: Transient, Actuator, Sensor, Biocomposite Plate, Delamination, Model Order Reduction.

1. INTRODUCTION

Recently, laminated composite structures are becoming widely used in aerospace and the automobile industry, because of their light weight and high stiffness/strength ratio, compared to metal materials. Especially, biocomposite laminates are highlighted because of their environmental friendly characteristics.¹ In spite of their strong advantages, the orthotropic material properties and complicated failure mechanism of laminated biocomposite structures still limit their general applications in major industries. Different material properties at each lamina generate difficulties in the analysis of laminated composite structures. The computational cost of full three-dimensional finite element analysis of laminated composite structure is very expensive. Therefore, quasi three-dimensional analysis techniques have been developed to analyze the laminated composite structures efficiently, such as zigzag theory,^{2–6} layerwise displacement theory,^{7–9} improved displacement theory,^{10,11} meshless

modeling,¹² asymptotic approach,^{13,14} and stress function based theory.^{15–17}

Delamination is one of the major failure mechanisms of laminated composite structures.^{18–21} The effects of delamination in laminated composite structures have been investigated based on zigzag theory for the bifurcation buckling²² and post buckling problem,^{23–26} in plate and shell structures. Dynamic characteristics of delaminated composite structures have also been investigated by the improved layerwise displacement theory.^{27,28}

Smart laminated composite structures have been spotlighted, because of their simple and easy implementation, and high performance in real applications.^{29–35} Actuators and sensors used in the smart structure can be applied to detect damage in laminated composite structures. Recently, Electro-active paper,^{36–44} IPMC,^{45,46} PVDF,^{47,48} and fullerene-reinforced Nafion^{49,50} have been highlighted as smart actuator and sensor materials.

To investigate the effects of delamination on the laminated composite structure, the modal strain-based damage index,⁵¹ and hybrid damage indicators,⁵² have been

* Author to whom correspondence should be addressed.

developed. Damage effects have also been quantified by the reliability method, using dimensional reduction, epistemic uncertainty, and adaptive sparse polynomial chaos expansion.^{53–57} In this research, transient responses of delaminated biocomposite laminates are analyzed, using the improved layerwise theory. To investigate the effect of delamination, piezoelectric actuators and sensors are modeled, and transient responses of piezoelectric sensor outputs are analyzed, to identify the damage effect in laminated biocomposite structures. The transient quasi-static Ritz vector method (TQSRV) that has been recently developed is incorporated, to improve the computational cost of problem solution.^{58–63}

It is an important issue to analyze the delamination of biocomposite laminates with the finite element procedure. With delamination, biocomposite laminates experiences deterioration of its stiffness, and the finite element procedure can be used to predict the transient responses of biocomposite structure, with and without, delamination. Nevertheless, as the size of the degrees of freedom of a biocomposite structure becomes huge, an efficient finite element procedure for transient and frequency responses should be developed. To resolve this difficulty, the currently developed model order reduction (MOR), called the transient quasi-static Ritz vector method, is employed,^{59–63} whose bases are Krylov subspace bases and eigenvectors, for efficient transient FE analysis. The employed MOR scheme shares the basic concepts with the established MOR schemes, that the structural responses in the time domain are spanned, or approximated, with “good” bases with a few unknown variables. In the TQSRV method, the bases of the multifrequency quasi-static Ritz vector method (MQSRV),⁶² and the mode superposition (MS) method are combined. The bases of the MQSRV method are calculated at multi-frequencies, and the bases of the MS method are some of the lowest eigenvectors of an FE model. By integrating the bases of the two schemes, depending on the simulation condition, it was found that they efficiently provide a considerably more accurate prediction for the structural responses of a complex FE model than the common MOR methods, in the prediction of responses with, and without, delamination of biocomposite structure.

2. PIEZOELECTRIC COMPOSITE STRUCTURE FORMULATION

2.1. Piezoelectricity

For an elastic system with piezoelectric materials, the total free energy F can be written as:

$$F(\varepsilon_{ij}E_i) = \frac{1}{2}C_{ijkl}\varepsilon_{ij}\varepsilon_{kl} - e_{ijk}E_i\varepsilon_{jk} - \frac{1}{2}b_{ij}E_iE_j \quad (1)$$

where, ε_{ij} are the components of the strain tensor, and E_i are the components of the electric field vector. The quantities c_{ijkl} and e_{ijk} represent elastic and piezoelectric

constants, respectively, and b_{ij} is the dielectric permittivity. Piezoelectric material with linear constitutive relations is considered in the present work. This implies constant material coefficients. The constitutive relations can be written as follows:

$$\begin{aligned} \sigma_{ij} &= \frac{\partial F}{\partial \varepsilon_{ij}} = c_{ijkl}\varepsilon_{kl} - e_{ijk}E_k \\ D_i &= -\frac{\partial F}{\partial E_i} = e_{ijk}\varepsilon_{jk} + b_{ij}E_j \end{aligned} \quad (2)$$

where, σ_{ij} and D_i are the components of the stress tensor and the electric displacement vector, respectively. Based on linear piezoelectricity, E_i is derivable from a scalar potential function ϕ , as follows:

$$E_i = -\phi_{,i} \quad (i = 1, 2, 3) \quad (3)$$

The equations of motion are now derived using variational principles, as follows.

$$\begin{aligned} \delta\pi_u &= -\int_0^{t_0} \int_V \rho \ddot{u}_i \delta u_i + \gamma \dot{u}_i \delta u_i + \sigma_{ij} \delta \varepsilon_{ij} dV dt \\ &+ \int_0^{t_0} \int_S t_i \delta u_i dS dt = 0 \end{aligned} \quad (4)$$

$$\delta\pi_\phi = -\int_0^{t_0} \int_V D_i \delta \phi_{,i} dV dt + \int_0^{t_0} \int_S q_e \delta \phi dS dt = 0$$

where, π_u and π_ϕ denote the energy functionals of mechanical and electrical fields, respectively. The quantities ρ and γ denote mass density and material damping constant, respectively. The quantity t_i represents the components of the traction vector, and q_e represents the charge density.

2.2. Improved Layerwise Theory with Delaminations

Accurate description of structural deformation is a key issue, in modeling biocomposite laminates of arbitrary thickness. The first-order shear deformation-based displacement field is used to address the overall response of the entire laminate, and layerwise functions are used to accommodate the complexity of zigzag-like in-plane deformation through the laminate thickness, while satisfying interlaminar shear stress continuity conditions. For model delamination, the assumed displacement field is supplemented with Heaviside unit step functions, which allow the introduction of an independent displacement field above and below the delamination.

Consider an N -layered laminated biocomposite plate with multiple delaminations. The displacements of a point with coordinates (x, y, z) are described using the superposition of first-order shear deformation and layerwise functions, as follows:

$$\begin{aligned} U_1^k(x, y, z, t) &= u_1 + A_1^k(z)\phi_1 + B_1^k(z)w_{,x} \\ &+ \bar{C}_1^j(z)\bar{w}_{,x}^j + \sum_{j=1}^{N-1} \bar{u}_1^j H(z - z_j) \end{aligned}$$

$$\begin{aligned}
 U_2^k(x, y, z, t) &= u_2 + A_2^k(z)\phi_2 + B_2^k(z)w_{,y} \\
 &\quad + \bar{C}_2^j(z)\bar{w}_{,y}^j + \sum_{j=1}^{N-1} \bar{u}_2^j H(z - z_j) \\
 U_3^k(x, y, z, t) &= w(x, y, t) + \sum_{j=1}^{N-1} \bar{w}^j(x, y, t) H(z - z_j)
 \end{aligned} \quad (5)$$

where, U_1^k and U_2^k denote in-plane displacement, and U_3^k denotes transverse deflection. The superscript k denotes the k -th layer of the laminate. The quantities u_1 , u_2 and w denote the displacement of the reference plane, and ϕ_1 and ϕ_2 are rotations of the normal to the reference plane about the x and y axes. The terms \bar{u}_1^j , \bar{u}_2^j and \bar{w}^j represent possible jumps in the displacement field, due to delamination allowing slipping and separation between upper and lower laminates, and z_j denotes the delaminated interface. The function $H(z - z_j)$ is the Heaviside unit step function. The layerwise functions $A_1^k(z)$, $B_1^k(z)$ and $\bar{C}_1^j(z)$ are obtained from the 4N constraint equations based on stress and displacement continuity at each lamina interface, and are expressed in term of laminate geometry and material properties ($i = 1, 2$).

2.3. Higher Order Piezoelectric Field

The field of electric potential must satisfy the surface boundary condition of applied voltages and the charge conservation law. Therefore, a cubic distribution of the potential field along the thickness of the piezoelectric layers is assumed. The potential field (ϕ^j) for the j -th layer can be written as follows.

$$\begin{aligned}
 \phi^j(x, y, z, t) &= \phi_0^j(x, y, t) - (z - z_0^j)E_z^j(x, y, t) + 4\left(\frac{z - z_0^j}{h^j}\right)^2 \\
 &\quad \times \left[(z - z_0^j)\left(\frac{\bar{\phi}^j(x, y, t)}{h^j} + E_z^j(x, y, t)\right) \right. \\
 &\quad \left. - \phi_0^j(x, y, t) \right] \quad (6)
 \end{aligned}$$

where, ϕ_0^j is the potential of a point in the mid-plane of the k -th piezoelectric layer. The quantity E_z^j denotes the electric field at mid-plane, and the term $-(z - z_0^j)E_z^j$ is used to address the linear potential distribution through the thickness. The quantity $\bar{\phi}^j$ denotes the potential difference between the top and the bottom electrodes covering the j -th piezoelectric transducer, and z_0^j and h^j denote the mid-plane position, and the thickness of the j -th piezoelectric layer, respectively.

2.4. Finite Element Implementation

A 4-noded plate element is used with linear Lagrange interpolation functions to describe the in-plane structural unknowns and electrical unknowns; and Hermite cubic interpolation functions are used for the out-of-plane unknowns. The primary displacement unknowns

and electric unknowns of the j -th piezoelectric layer are expressed in terms of nodal values and shape functions, as follows:

$$\begin{aligned}
 (u_1, u_2, \phi_1, \phi_2, \bar{u}_1^j, \bar{u}_2^j) \\
 = \sum_{m=1}^4 N_m [(u_1)_m, (u_2)_m, (\phi_1)_m, (\phi_2)_m, (\bar{u}_1^j)_m, (\bar{u}_2^j)_m] \\
 w = \sum_{m=1}^4 \{H_m(w)_m + H_{xm}(w_{,x})_m + H_{ym}(w_{,y})_m\} \quad (7) \\
 \bar{w}^j = \sum_{m=1}^4 \{H_m(\bar{w})_m + H_{xm}(\bar{w}_{,x})_m + H_{ym}(\bar{w}_{,y})_m\} \\
 (\phi_0^j, E_z^j) = \sum_{m=1}^4 N_m [(\phi_0^j)_m, (E_z^j)_m]
 \end{aligned}$$

where, N_m is a Lagrange interpolation function and H_m , H_{xm} and H_{ym} are Hermite interpolation functions. The relationship between displacement unknowns and nodal unknowns in Eq. (7) can be expressed by the following matrix form:

$$\begin{aligned}
 \{u_u^e\} &= [N_u] \{d_u\} \\
 \{u_\phi^e\} &= [N_\phi] \{d_\phi\} \quad (8)
 \end{aligned}$$

Substituting Eq. (8) into Eq. (4), the standard equations of motion are obtained, and are written in matrix form, as follows:

$$\begin{aligned}
 \mathbf{M}_{uu} \ddot{\mathbf{d}}_u + \mathbf{C}_{uu} \dot{\mathbf{d}}_u + \mathbf{K}_{uu} \mathbf{d}_u + \mathbf{K}_{u\phi} \mathbf{d}_\phi &= \mathbf{F}_u \\
 \mathbf{K}_{\phi u} \mathbf{d}_u + \mathbf{K}_{\phi\phi} \mathbf{d}_\phi &= \mathbf{F}_\phi \quad (9)
 \end{aligned}$$

where, \mathbf{d}_u denotes the displacement unknowns of the element, and \mathbf{d}_ϕ denotes the electrical unknowns of the piezoelectric layer. The structural mass matrix and the damping matrix are denoted by \mathbf{M}_{uu} and \mathbf{C}_{uu} , respectively. The structural stiffness matrix, the coupled stiffness matrix, and the electric stiffness matrix are denoted by \mathbf{K}_{uu} , $\mathbf{K}_{\phi u}$ and $\mathbf{K}_{\phi\phi}$, respectively. The structural force and the electric force are denoted by \mathbf{F}_u and \mathbf{F}_ϕ , respectively.

Without loss of generality, the time varying response of the developed finite element formulations of Eq. (9) with time varying force can be defined by Newton's second equation, as follows:

$$\mathbf{M}\ddot{\mathbf{X}} + \mathbf{C}\dot{\mathbf{X}} + \mathbf{K}\mathbf{X} = \mathbf{F}, \quad \mathbf{X} = [\mathbf{d}_u, \mathbf{d}_\phi]^T \quad (10)$$

$$\begin{aligned}
 \mathbf{M} &= \begin{pmatrix} \mathbf{M}_{uu} & \mathbf{0} \\ \mathbf{0} & \mathbf{0} \end{pmatrix}, \quad \mathbf{K} = \begin{pmatrix} \mathbf{K}_{uu} & \mathbf{K}_{u\phi} \\ \mathbf{K}_{\phi u} & \mathbf{K}_{\phi\phi} \end{pmatrix}, \\
 \mathbf{C} &= \begin{pmatrix} \mathbf{C}_{uu} & \mathbf{0} \\ \mathbf{0} & \mathbf{0} \end{pmatrix} \quad (11)
 \end{aligned}$$

where, the vector migrating the structural displacements and the electric potential vector is \mathbf{X} . The velocity and the acceleration vectors are denoted by $\dot{\mathbf{X}}$ and $\ddot{\mathbf{X}}$, respectively.

To solve the above finite element equations, the following Newmark scheme can be adopted:

$$\ddot{\mathbf{X}}_0 = \mathbf{M}^{-1}(\mathbf{F}_0 - \mathbf{K}\mathbf{X}_0 - [\mathbf{C}]\dot{\mathbf{X}}_0) \quad (12)$$

$$\mathbf{K}_{\text{Eff}}\mathbf{X}_{n+1} = \mathbf{F}_{n+1}^{\text{Eff}} \quad (13)$$

$$\mathbf{K}_{\text{Eff}} = \mathbf{K} + \frac{1}{\beta(\Delta t)^2}\mathbf{M} + \frac{\gamma}{\beta(\Delta t)}\mathbf{C} \quad (14)$$

$$\begin{aligned} \mathbf{F}_{n+1}^{\text{Eff}} = & \mathbf{F}_{n+1} + \mathbf{M}\left\{\frac{1}{\beta(\Delta t)^2}\mathbf{X}_n + \frac{1}{\beta(\Delta t)}\dot{\mathbf{X}}_n + \left(\frac{1}{2\beta} - 1\right)\ddot{\mathbf{X}}_{n+1}\right\} \\ & + \mathbf{C}\left\{\frac{\gamma}{\beta(\Delta t)}\mathbf{X}_n + \left(\frac{\gamma}{\beta} - 1\right)\dot{\mathbf{X}}_n\right. \\ & \left. + \Delta t\left(\frac{\gamma}{2\beta} - 1\right)\ddot{\mathbf{X}}_n\right\} \end{aligned} \quad (15)$$

$$\ddot{\mathbf{X}}_{n+1} = \frac{1}{\beta\Delta t^2}(\mathbf{X}_{n+1} - \mathbf{X}_n) - \frac{1}{\beta\Delta t}\dot{\mathbf{X}}_n - \left(\frac{1}{2\beta} - 1\right)\ddot{\mathbf{X}}_n \quad (16)$$

$$\dot{\mathbf{X}}_{n+1} = \dot{\mathbf{X}}_n + \Delta t(1 - \gamma)\ddot{\mathbf{X}}_n + \gamma\Delta t\ddot{\mathbf{X}}_{n+1} \quad (17)$$

where, the effective stiffness matrix, the effective force at the $(n+1)$ th time step and the external force of the $(n+1)$ th time step of the Newmark scheme are denoted by \mathbf{K}_{Eff} , $\mathbf{F}_{n+1}^{\text{Eff}}$, and \mathbf{F}_{n+1} , respectively. The external force at the 0th time step is \mathbf{F}_0 . Note that by assuming the constant time increment step, the effective stiffness matrix, \mathbf{K}_{Eff} , becomes constant during the time integration procedure.

2.5. Transient Quasi-Static Ritz Vector Method

By approximating the original structural response with the approximated response, $\Psi\mathbf{Q}$, the MOR methods reduce the size of the linear algebra system, by transforming a large set of system equations into a small set of equations. From a mathematical point of view, the approximated response, \mathbf{X}_A , of the original response \mathbf{X} can be defined as follows:^{59–63}

$$\mathbf{A}\mathbf{X} = \mathbf{B} \quad (18)$$

$$\mathbf{X} \cong \mathbf{X}_A = \Psi\mathbf{Q} \quad (19)$$

$$\Psi = [\varphi_1, \varphi_2, \dots, \varphi_{n_d}] \quad (n_d \leq n_s) \quad (20)$$

where, \mathbf{A} and \mathbf{B} denote an arbitrary $n_s \times n_s$ system matrix and a $n_s \times 1$ force vector that vary, depending on the mechanical system of interest. The number of degrees of freedom of a system is n_s . In Eq. (19), Ψ is the frequency dependent basis vector of order n_d , and \mathbf{Q} are the retained unknown variables for the basis. By pre-multiplying Ψ^T into the original dynamic Eq. (18), the following reduced equation with order n_d is obtained.

$$\underbrace{\{\Psi^T \mathbf{A} \Psi\}}_{n_d \times n_d} \underbrace{\mathbf{Q}}_{n_d \times 1} = \underbrace{\Psi^T \mathbf{B}}_{n_d \times 1} \quad (21)$$

By solving the above reduced system with order n_d for \mathbf{Q} , the approximate solution \mathbf{X}_A is recovered, using Eq. (19). Note that as the MOR scheme has been

developed mainly to reduce the computational time, most relevant researches explain the concepts of the MOR schemes for the frequency response function. But recently, a new MOR scheme for transient FE analysis, called the transient quasi-static Ritz vector method (TQSRV), was developed.⁶³ How to calculate proper bases for the MOR scheme of a transient FE system is an important question. In the transient quasi-static Ritz vector method, we combine the bases of the MQSRV method, generating Krylov subspace bases at multiple frequencies, and the bases of the MS method, together, as follows:

$$\begin{aligned} \mathbf{Q} = & \left[\underbrace{\varphi_{1,1} \dots \varphi_{n_d,1}}_{\text{Krylov subspace at the 1st frequency domain}} \dots \underbrace{\varphi_{1,nf} \dots \varphi_{n_d,nf}}_{\text{Krylov subspace at the nf frequency domain}} \right] \\ & \cup [\varphi_{\text{eigen-modes}}] \end{aligned} \quad (22)$$

where, the mass orthogonalized bases of the multifrequency quasi-static Ritz vector method for the i -th base at the s -th center angular velocity are denoted by $\varphi_{i,s}$. The number of bases at the s th center frequencies is $n_{d,s}$. The several eigenvectors orthogonalized with the MQSRV bases are denoted by $\varphi_{\text{eigen-modes}}$. The reason for the above combined bases is that the Krylov subspace bases at multifrequencies are effective in a wide range of frequency domains, and the eigenvector bases are also appropriate, in approximating the transient motions of structural parts. After calculating the above bases of the TQSRV method, the standard reduction process is applied for the Newmark process. The algorithm of the Newmark scheme with the present TQSRV method is given in Table I.

$$n_{d,\text{total}} = \sum_{k=1}^{nf} n_{d,k} + n_{d,\text{eig}} \quad (23)$$

$$\underbrace{\mathbf{K}_{\text{Eff}}^{\text{MOR}}}_{n_{d,\text{total}} \times n_{d,\text{total}}} = \underbrace{\Phi^T}_{n_d \times n_d} \underbrace{\mathbf{K}_{\text{Eff}}}_{n \times n} \underbrace{\Phi}_{n \times n_{d,\text{total}}} , \underbrace{\mathbf{F}_{\text{Eff}}^{\text{MOR}}}_{n_{d,\text{total}} \times 1} = \underbrace{\Phi^T}_{n_d \times n_d} \underbrace{\mathbf{F}_{n+1}^{\text{Eff}}}_{n \times 1} \quad (24)$$

$$\mathbf{K}_{\text{Eff}}^{\text{MOR}} \mathbf{Q}_{n+1} = \mathbf{F}_{\text{Eff}}^{\text{MOR}} \quad (25)$$

$$\begin{aligned} \ddot{\mathbf{Q}}_{n+1} = & \left(\frac{1}{\beta\Delta t^2}(\mathbf{Q}_{n+1} - \mathbf{Q}_n) \right. \\ & \left. - \frac{1}{\beta\Delta t}\dot{\mathbf{Q}}_n + \left(\frac{1}{2} - \beta\right)\ddot{\mathbf{Q}}_n \right) \end{aligned} \quad (26)$$

Table I. The Newmark scheme with the present TQSRV method.

Calculate the reduction bases
Calculate the reduced initial position, the reduced velocity, and the reduced acceleration
Calculate the reduced effective stiffness matrix
For a time step
Calculate the current force and the reduced force
Calculate the reduced displacements
Update the reduced accelerations
Update the reduced velocities
end

$$\dot{\mathbf{Q}}_{n+1} = \dot{\mathbf{Q}}_n + \Delta t(1 - \gamma)\ddot{\mathbf{Q}}_n + \gamma\Delta t\ddot{\mathbf{Q}}_{n+1} \quad (27)$$

$$\mathbf{X}_{n+1} = \Phi\mathbf{Q}_{n+1}, \dot{\mathbf{X}}_{n+1} = \Phi\dot{\mathbf{Q}}_{n+1}, \ddot{\mathbf{X}}_{n+1} = \Phi\ddot{\mathbf{Q}}_{n+1} \quad (28)$$

It should be noted that rather than the backward and forward substitutions of the LU decomposition of the effective stiffness matrix, K_{Eff} , or a direct matrix inversion, the inversion of a small size matrix, $K_{\text{Eff}}^{\text{MOR}}$, is formulated, and the displacement, velocity and acceleration updates are also performed in the reduced space in (27).

3. RESULTS AND DISCUSSION

The transient analysis of delaminated biocomposite plate is conducted using the proposed theory, to illustrate the effects of delamination, with and without MOR. A cross-ply hemp/cellulose acetate biocomposite laminates,¹ with symmetric stacking sequence $([0/90]_{4s})$ is studied. The dimensions of the cantilever plates are 30 cm length, 5 cm width and 0.2 cm thickness. One piezoelectric actuator and one piezoelectric sensor are used to excite the composite plate, and to detect the structural response. Both the actuator and the sensor are surface bonded to the plate. The size of the actuator is 3 cm \times 3 cm \times 0.025 cm. The actuator is located 1 cm apart from the root. A piezoelectric sensor, surface bonded at a distance of 6 cm away from the fixed end, is used to detect the voltage output, when the external loads from the actuator excite the plate. The size of the piezoelectric sensor is 1 cm \times 1 cm \times 0.025 cm. A delamination of size 10 cm \times 5 cm is seeded at a distance of 10 cm from the fixed end. Three different locations of delamination through the thickness direction are considered. Case 1 (D0) is that the delamination is located at the mid-surface. The delamination is located at the third interface from the mid surface for case 2 (D3), and at the sixth interface for case 3 (D6). The geometry of the

Table II. Material Properties of PZT 5A and biocomposites.

Hemp/cellulose acetate biocomposite lamina		PZT 5A	
E1	5.8 GPa	E	69 GPa
E2	4.69 GPa	ν	0.31
G12	0.99 GPa	ρ	7700 Kg/m ³
ρ	1300 Kg/m ³	d_{31}	179 pC/N
ν_{12}	0.3	d_{32}	179 pC/N
ν_{13}	0.3	b_{33}	9.53 nF/m

delaminated biocomposite plate is shown in Figure 1. The material properties for the laminated biocomposites and PZT 5A are given in Table II.

To study the efficiency of the MOR for damage analysis of laminated biocomposite plate, the plate is excited by an actuator impulse load of 100 Volt for 1 milliseconds. A finite element mesh consisting of 120 by 20 four-noded plate elements is used in the numerical analysis.

Figure 2 shows a comparison of tip displacement and sensor voltage output for healthy plate with, and without, the TQSRV method. The transient responses obtained by full analysis and the MOR in Figure 2 show exactly the same time history. The order of magnitude of the absolute error between the responses of the full analysis and the TQSRV method is under 10^{-6} , and this illustrates that the TQSRV method can exactly reproduce the structural response of the full analysis. Figure 2(b) shows the sensor outputs calculated by both methods. As expected, the sensor outputs are fairly matched with the structural response. The sensor outputs also show the same trend and magnitude between the full analysis and the TQSRV method. The order of magnitude of the absolute error between full analysis and the TQSRV method is about 10^{-6} in the beginning, but reduces to 10^{-10} .

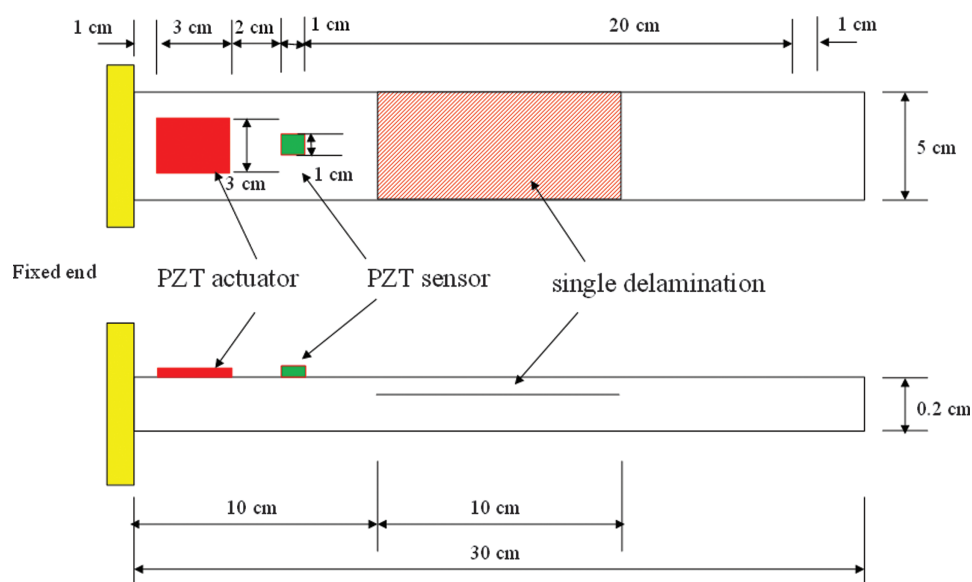


Figure 1. Geometry of the delaminated smart composite plate.

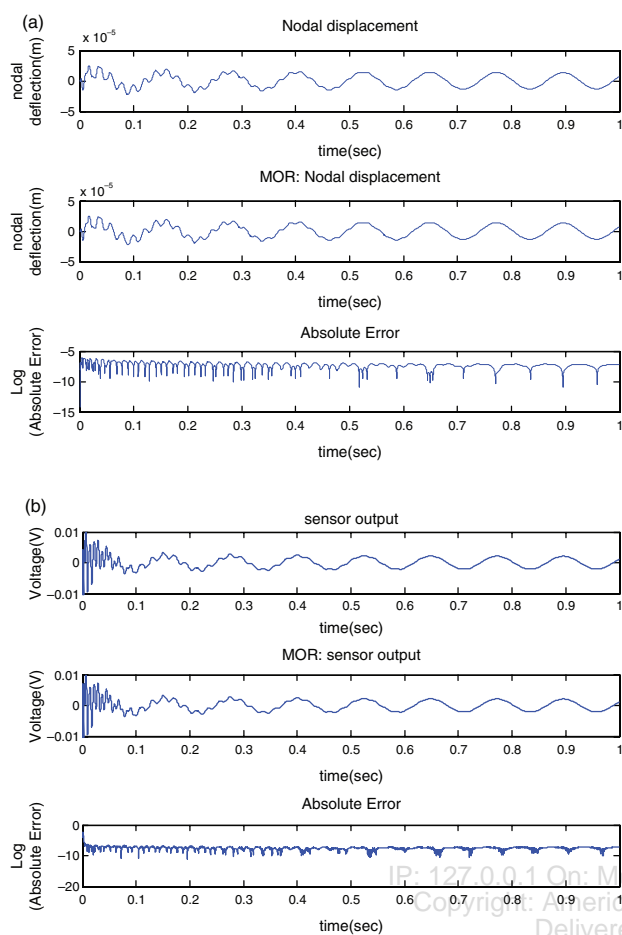


Figure 2. Comparison of the structural and sensor voltage output of full Newmark analysis and TQSRV analysis. (a) Structural displacements, and (b) sensor voltage output for the healthy plate.

Figure 3 shows the comparisons of the tip displacement and the sensor output for the delaminated plate (D0) with, and without, the TQSRV method. The transient responses obtained by full analysis and the TQSRV method show almost the same time histories, with sufficient accuracy to use it from an engineering point of view. Figure 3(b) shows the sensor outputs calculated by the full analysis and the TQSRV method. The sensor outputs also show the same trend and magnitude between full analysis and the TQSRV method. The order of magnitude of absolute error between full analysis and MOR is 10^{-7} in the average sense.

Figures 4 and 5 show comparisons of the power spectral density (PSD) with, and without, the MOR calculated by the transient response of structural and sensor voltage output of healthy, and three delaminated, biocomposite plates. The order of magnitude of absolute error between full analysis and the TQSRV method in transient response is almost zero, therefore the PSDs of healthy and delaminated plates are almost exactly the same with, and without, the TQSRV method. Although the delamination effects are not clear in the transient structural response and sensor output, the damage effects are clearly observed in these

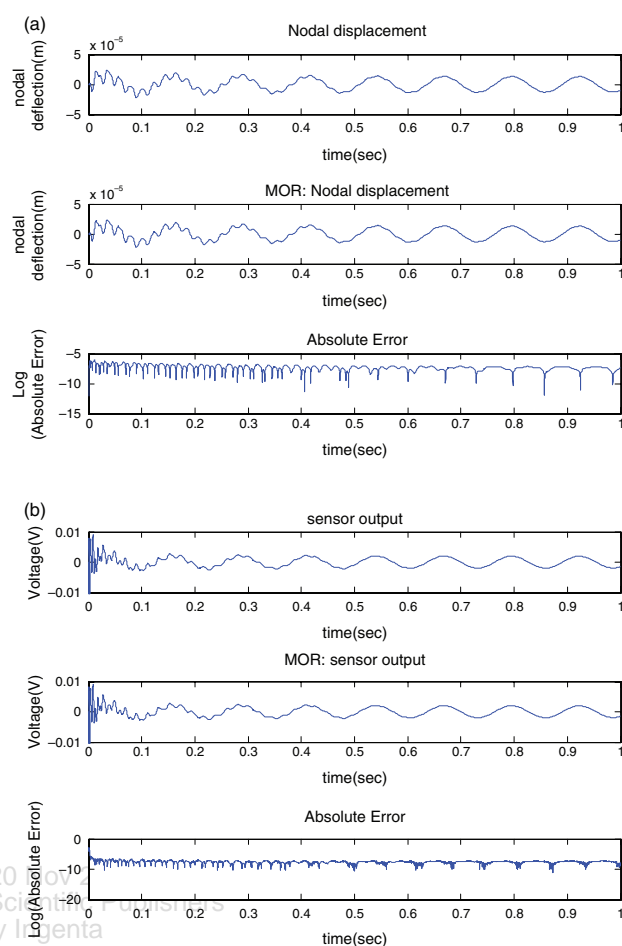


Figure 3. Comparison of the structural and sensor voltage output of full Newmark analysis and TQSRV analysis. (a) Structural displacements, and (b) sensor voltage output for delaminated plate (D0).

PSDs: the deteriorations of the stiffness of the delaminated biocomposite structure. In Figures 4 and 5, the delamination case (D0) shows the largest natural frequency down shift that implies the largest damage effect, with the delamination located at the mid surface of the plate.

More importantly, Table III represents speedup of the TQSRV method, compared to the full Newmark scheme.

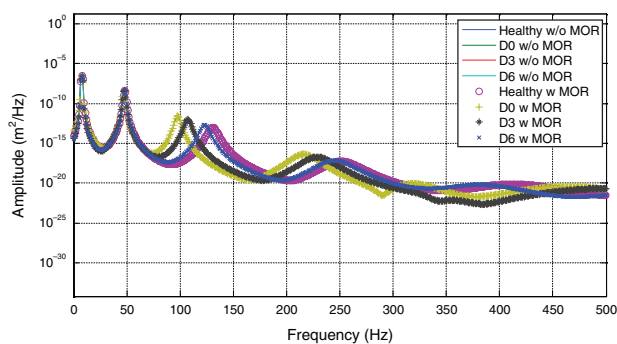


Figure 4. Comparison of power spectral density from nodal displacements for healthy and delaminated plates.

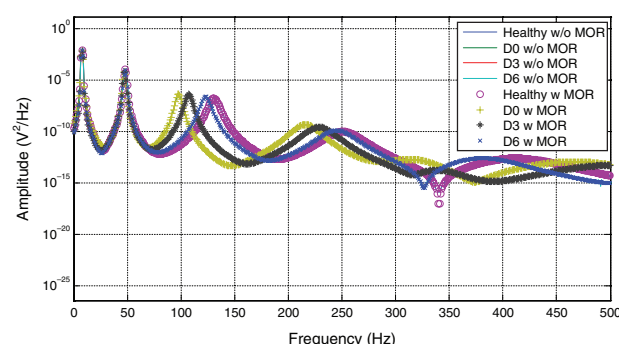


Figure 5. Comparison of power spectral density from sensor voltage output for healthy and delaminated plates.

Table III. Speedup of the TQSRV method for the FE analyses of healthy and delaminate plates.

Damage case	Size of effective stiffness matrix/condition number	Full Newmark scheme (sec)	TQSRV method (sec)	Speedup
Healthy	17787/4.0275 × 10 ¹⁷	39932	478	83.46
D0	22092/7.6594 × 10 ¹⁹	40327	523	77.10
D3	22092/5.6743 × 10 ¹⁷	40103	311	128.75
D6	22092/4.2075 × 10 ¹⁶	44056	353	123.75

The computational costs of TQSRV are 0.78% to 1.3%, compared to the full Newmark scheme. As the matrix condition number of case D0 is bad, the TQSRV method takes more time. It is also expected that if the size of matrix is increased, this speedup will increase.

4. CONCLUSION

Transient analysis of delaminated biocomposite structures has been conducted, using the full Newmark-beta algorithm and TQSRV. The displacement field of the laminated biocomposite plate was modeled using an improved layerwise displacement theory. Delamination was modeled using the Heaviside unit step function, and higher order electric potential provided an accurate actuator and sensor model. The transient response of structural node and sensor output showed not enough information of delamination, but the power spectral density of the time history provided the clear effects of delamination. The MOR predicted almost the same transient response as that calculated by full Newmark-beta analysis. The order of magnitude of absolute error between full analysis and the MOR is 10⁻⁷. The computational cost of TQSRV is around 1% of full Newmark-beta analysis. TQSRV is proved as a powerful method to analyze the transient response of delaminated biocomposite structures.

Acknowledgment: This research was supported by the Basic Science Research Program, through the National Research Foundation of Korea (NRF), funded by the Ministry of Education, Science and Technology (NRF-2011-0021720 and No. 2012R1A1A2A10038803).

References and Notes

- J. C. Sarah and B. Sarah, Technical Report No. 168, Stanford University (2009).
- J. Oh, M. Cho, and J. S. Kim, *Smart Mater. Struct.* 16, 2229 (2007).
- J. S. Kim and M. Cho, *Int. J. Solids Struct.* 44, 1256 (2007).
- J. S. Kim, *J. Sound Vibr.* 308, 268 (2007).
- J. S. Kim, *Aiaa J.* 42, 1685 (2004).
- M. Cho and J. S. Kim, *Aiaa J.* 35, 587 (1997).
- I. Lee, J. H. Roh, and I. K. Oh, *J. Therm. Stresses* 26, 525 (2003).
- I. K. Oh, *Compos. Pt. B-Eng.* 38, 159 (2007).
- J. H. Roh, I. K. Oh, S. M. Yang, J. H. Han, and I. Lee, *Smart Mater. Struct.* 13, 1337 (2004).
- X. Zhou, A. Chattopadhyay, and H. S. Kim, *J. Reinf. Plast. Compos.* 23, 131 (2004).
- H. S. Kim, X. Zhou, and A. Chattopadhyay, *Aiaa J.* 40, 2517 (2002).
- S. Singh, J. Singh, and K. K. Shukla, *J. Mech. Sci. Technol.* 27, 327 (2013).
- J. S. Kim, M. Cho, and E. C. Smith, *Int. J. Solids Struct.* 45, 1954 (2008).
- J. Jeong, J. S. Kim, Y. J. Kang, and M. Cho, *J. Mech. Sci. Technol.* 26, 161 (2012).
- H. S. Kim, M. Cho, and G. I. Kim, *Compos. Struct.* 49, 229 (2000).
- M. Cho and H. S. Kim, *Int. J. Solids Struct.* 37, 435 (2000).
- S. Y. Rhee, M. Cho, and H. S. Kim, *Int. J. Solids Struct.* 43, 4757 (2006).
- H. S. Kim, A. Chattopadhyay, and A. Ghoshal, *Comput. Struct.* 81, 1555 (2003).
- H. S. Kim, A. Ghoshal, A. Chattopadhyay, and W. H. Prosser, *J. Reinf. Plast. Compos.* 23, 1207 (2004).
- A. Chattopadhyay, H. S. Kim, and A. Ghoshal, *J. Sound Vibr.* 273, 387 (2004).
- H. S. Kim, A. Ghoshal, J. Kim, and S. B. Choi, *Smart Mater. Struct.* 15, 221 (2006).
- M. Cho and J. S. Kim, *Aiaa J.* 35, 268 (2007).
- J. S. Kim and M. Cho, *Int. J. Numer. Methods Eng.* 55, 1323 (2002).
- J. Oh, M. Cho, and J. S. Kim, *Finite Elem. Anal. Des.* 44, 675 (2008).
- J. S. Kim and M. Cho, *Aiaa J.* 41, 941 (2003).
- J. S. Kim and M. Cho, *Aiaa J.* 37, 774 (1999).
- H. S. Kim, A. Chattopadhyay, and A. Ghoshal, *Aiaa J.* 41, 1771 (2003).
- A. Ghoshal, H. S. Kim, A. Chattopadhyay, and W. H. Prosser, *Finite Elem. Anal. Des.* 41, 850 (2005).
- H. S. Kim, A. Chattopadhyay, and C. H. Nam, *J. Intell. Mater. Syst. Struct.* 13, 713 (2002).
- S. B. Choi, H. S. Kim, and J. S. Park, *J. Sound Vibr.* 300, 160 (2007).
- L. J. Zhao, H. S. Kim, and J. Kim, *Aiaa J.* 45, 79 (2007).
- L. J. Zhao, H. S. Kim, and J. Kim, *J. Mech. Sci. Technol.* 21, 642 (2007).
- H. S. Kim, J. H. Kim, and J. Kim, *Int. J. Precis. Eng. Manuf.* 12, 1129 (2011).
- J. Kim and H. S. Kim, *J. Mech. Sci. Technol.* 23, 452 (2009).
- I. K. Oh, *Smart Mater. Struct.* 14, 823 (2005).
- J. Kim, H. Lee, and H. S. Kim, *Int. J. Precis. Eng. Manuf.* 11, 823 (2010).
- G. Y. Yun, H. S. Kim, and J. Kim, *Smart Mater. Struct.* 17, 025021 (2008).
- G. Y. Yun, H. S. Kim, J. Kim, K. Kim, and C. Yang, *Sens. Actuator A-Phys.* 141, 530 (2008).
- H. S. Kim, Y. Li, and J. Kim, *Sens. Actuator A-Phys.* 147, 304 (2008).
- H. Kim, C. Yang, and J. Kim, *J. Mech. Sci. Technol.* 23, 2285 (2009).
- J. Kim, W. Jung, and H. S. Kim, *Sens. Actuator A-Phys.* 140, 225 (2007).
- H. S. Kim, J. Kim, W. Jung, J. Ampofo, W. Craft, and J. Sankar, *Smart Mater. Struct.* 17, 015029 (2008).
- J. Kim, J. Ampofo, W. Craft, and H. S. Kim, *Mech. Mater.* 40, 1001 (2008).

44. C. Yang, J. H. Kim, J. H. Kim, J. Kim, and H. S. Kim, *Sens. Actuator A-Phys.* 154, 117 (2009).
45. J. H. Jeon and I. K. Oh, *Thin Solid Films* 517, 5288 (2009).
46. V. Sridhar, J. H. Jeon, and I. K. Oh, *Carbon* 48, 2953 (2010).
47. X. L. Wang, I. K. Oh, and J. B. Kim, *Compos. Sci. Technol.* 69, 2098 (2009).
48. J. H. Jeon, S. P. Kang, S. Lee, and I. K. Oh, *Sens. Actuator B-Chem.* 143, 357 (2009).
49. J. H. Jung, J. H. Jeon, V. Sridhar, and I. K. Oh, *Carbon* 49, 1279 (2011).
50. J. H. Jung, S. Vadahanambi, and I. K. Oh, *Compos. Sci. Technol.* 70, 584 (2010).
51. H. S. Kim, J. Kim, S. B. Choi, A. Ghoshal, and A. Chattopadhyay, *Aiaa J.* 45, 2972 (2007).
52. A. Ghoshal, H. S. Kim, J. Kim, S. B. Choi, W. H. Prosser, and H. Tai, *Finite Elem. Anal. Des.* 42, 715 (2006).
53. C. Hu and B. D. Yoon, *Struct. Multidiscip. Optim.* 43, 419 (2011).
54. B. D. Yoon, K. K. Choi, L. Du, and D. Gorsich, *J. Mech. Des.* 129, 876 (2007).
55. C. Hu, B. D. Yoon, and J. Chung, *Appl. Energy* 92, 694 (2012).
56. B. D. Yoon and Z. M. Xi, *Struct. Multidiscip. Optim.* 37, 475 (2009).
57. J. H. Choi, W. H. Lee, J. J. Park, and B. D. Yoon, *Struct. Multidiscip. Optim.* 35, 531 (2008).
58. H. G. Kim and M. Cho, *J. Mech. Sci. Technol.* 27, 113 (2013).
59. J. S. Han, E. B. Rudnyi, and J. G. Korvink, *J. Micromech Microeng* 15, 822 (2005).
60. Z. D. Ma, N. Kikuchi, and I. Hagiwara, *Computational Mechanics* 13, 157 (1993).
61. G. H. Yoon, *Comput. Meth. Appl. Mech. Eng.* 199, 1744 (2010).
62. G. H. Yoon, *Int. J. Numer. Methods Eng.* 89, 1451 (2012).
63. G. H. Yoon, MSD Lab Report, Hanyang University (2013).

Received: 21 May 2013. Accepted: 20 October 2013.

IP: 127.0.0.1 On: Mon, 20 Nov 2023 02:39:42
Copyright: American Scientific Publishers
Delivered by Ingenta